Available online at www.sciencedirect.com

ScienceDirect

ELSEVIER

materialstoday: PROCEEDINGS

International Conference on Advances in Materials Science, Communication and Microelectronics (ICAMCM-2021)

Study of the effects of annealing temperature on the properties of piezoelectric *ZnO* thin film for the development of MEMS acoustic sensor

Washim Reza Ali[a,b,*], Anshuman Raunak[a,b] and Mahanth Prasad[a,b]

[a] *CSIR-Central Electronics Engineering Research Institute, Pilani – 333031, India*
[b] *Academy of Scientific and Innovative Research (AcSIR), Ghaziabad- 201002, India*

Abstract

This paper reports deposition and characterization of Zinc oxide (ZnO) thin film to be used as sensing layer in an acoustic sensor. An important requirement for such devices is the presence of high *c*-axis orientation and low stress in the deposited *ZnO* film. For this purpose, annealing of the deposited films is very much necessary. Here, zinc oxide thin films have been deposited over oxidized *Si*(100) wafer using radiofrequency (*RF*) magnetron sputtering method and are annealed at different temperatures from $200 - 400°C$ in steps of $50°C$. Different microstructural parameters such as grain size, surface roughness, dislocation density and stress have been determined to obtain the optimized annealing temperature for the thin film. The optimization of the annealing temperature is necessary to obtain ZnO thin film with better piezoelectric response. Surface roughness has also been determined from *AFM* measurements. The *XRD* study indicates that the intensity of (002) peak changes with annealing temperature. Grain size increases from $15.46nm$ to $18.24nm$ and dislocation density decreases to minimum value $\sim 3.006 \times 10^{-3} nm^{-2}$ as temperature is increased to $400°C$. Stress is also minimum at temperatures of $350 - 400°C$. An annealing temperature of approx. 350° C has been found to be optimum for *ZnO* film to be used in acoustic sensor.

Keywords: Acoustic sensor, Annealing, ZnO, stress, dislocation density, grain size;

1. Introduction

Most of the micro-electromechanical systems (MEMS)-based acoustic sensors have been developed for audio applications that normally require a maximum *SPL* of *120dB* and bandwidths of *20kHz* [1-8]. Among the commonly used transduction mechanisms of capacitive, piezoresistive and piezoelectric, piezoelectric transduction offers advantages of durability, high sensitivity, low noise and also it has no power requirement for its operation [9]. Generally, in MEMS, thin film devices are preferred over their bulk counterparts due to the inherent advantages in device design flexibility and also due to the feasibility of integration in complex systems [10]. In recent years, *ZnO* has become one of most widely used piezoelectric thin films for a variety of applications in MEMS such as film-bulk acoustic-wave resonators, *SAW* resonators and acousto-electric devices [11]. Thin film *ZnO* layers can be deposited by using physical vapour deposition (PVD) methods [12-13], evaporation [14], sol-gel processing [15-16] and metal-organic chemical vapour deposition (MOCVD) [17]. However, among these, sputtering [18-19] have been extensively used to deposit *c*-axis oriented *ZnO* layers due to its ease of operation, good repeatability, option of

---

* Corresponding author. Tel. +91-8472820359, *E-mail address:*rezali786@gmail.com

deposition at low temperature and compatibility with standard *Si*- fabrication technology.

Mechanical stress arises in thin films due to its deposition on a substrate. This stress results from two factors–one arises from the differences in coefficients of thermal expansion (CTE) of piezo-electric thin film and the underlying layer and the other one arises from the existence of structural imperfections such as grain boundaries, vacancies etc. in the thin film [11]. However, intrinsic stress arising from the *ZnO* thin film growth process causes the phase velocity in acoustic wave devices to change significantly. Moreover, stressed *ZnO* films exhibit relaxation behavior with time, causing aging effects which alter the specifications of the device [20]. Furthermore, presence of intrinsic stress gives rise to a static transverse deflection even in the absence of an applied pressure which greatly affects the sensitivity of the device [21]. Therefore, deposition of a stress-free or low stress ZnO film is essential for acoustic devices. Moreover, reduction in dislocation density or increase in grain size greatly improves the crystallinity of the film which in turn enhances its piezoelectric performance. All of these can be achieved through proper application of post-deposition annealing. Therefore, in the present approach, annealing temperature optimization has been done to obtain minimum stress, dislocation density, increased grain size and enhanced crystallinity of the *ZnO* thin film to be used in an acoustic sensor.

ZnO thin film was deposited using *RF* reactive magnetron sputtering system using a *Zn* metal target of 99.99% purity and O_2 supply. The deposition was carried out at room temperature without any substrate heating. The optimized deposition rate was $7nm/min$ and after 6hrs, a thickness of $2.5\ \mu m$ was obtained. Table 1 is showing the deposition parameters used for sputtering. Deposited samples were then annealed for 1hr at different annealing temperatures ranging from $200 - 400^oC$ in steps of 50^oC in O_2 ambient. The structural and morphological studies were carried out using an *X*-ray diffractometer (Rigaku) and Atomic Force Microscope (Veeco), respectively. Grain size, strain and stress were calculated from *XRD* spectrum and surface roughness from *AFM* image.

Table 1. Deposition parameters for *ZnO* thin film

Parameters	Values
RF power	$400W$
Working Pressure	$20mTorr$
Gas flow rate	$Ar:\ 20sccm$ $O_2:\ 30sccm$
Substrate temperature	*No heating*
Deposition rate	$7nm/min$
Distance between target and substrate	$10cm$

2. Proposed fabrication process flow

The basic process flow of the proposed acoustic device can be summarized as- (i) selection of Si wafers and cleaning using $RCA1$ (NH_3 (29%) : H_2O_2(30%) : DI water = $1:1:5$) and $RCA2$ (HCl(37%) : H_2O_2(30%): DI water = $1:1:6$); (ii) fabrication of micro-hole/tunnel for pressure compensation and thereafter, bulk micromachining to release diaphragm; thermal oxidation to grow a thin insulating oxide layer; (iii) deposition of bottom electrode of *Au* using sputtering and subsequent etching; (iv) deposition of thin *PECVD* oxide; (v) deposition of piezoelectric layer of *ZnO* using sputtering and subsequent etching; (vi) again thin *PECVD* oxide layer deposition along with top electrode of *Au* deposition by sputtering and then etching followed by *RIE* to open the pads and finally, anodic bonding with pyrex glass to seal the cavity. Fig. 1 is showing the complete fabrication process flow.

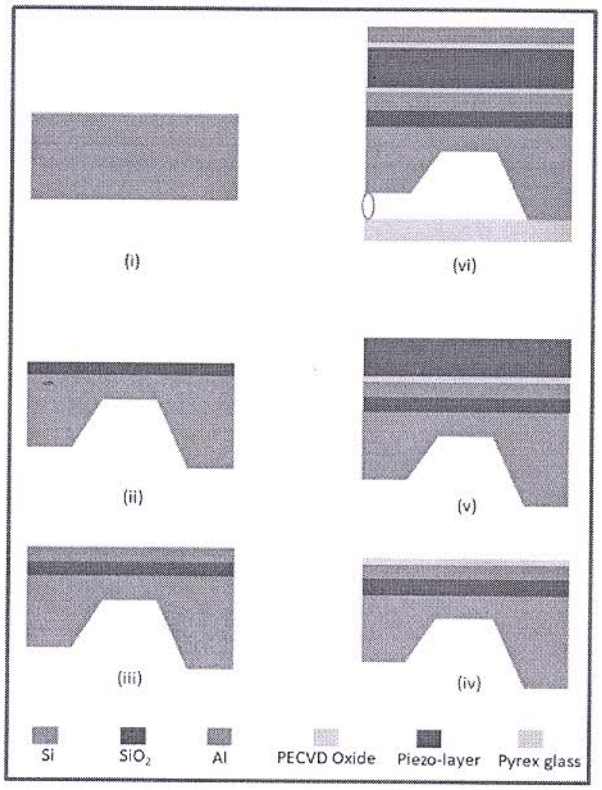

Fig. 1. Fabrication process flow.

3. Result & Discussion

Crystallographic characteristics of the as-deposited and annealed films have been studied using *XRD*. With the increase in annealing temperature from $200-400^{o}$ C, the intensity of peaks has also increased, indicating an enhanced crystallinity (Fig. 2(a)). The high annealing temperature provides energy to the film atoms which enhances their mobility that in turn leads to decrease in defects in the *ZnO* films. This improves the film quality and hence the enhanced crystallinity [22-23]. Defect free thin film with enhanced crystallinity indicates improved performance of sensor. The (002) peak position of *ZnO* powder is $2\theta = 34.448^{o}$. However, in our deposited *ZnO* films, there is deviation in the position of the diffraction peak from its powder value. The position shifting indicates a decrease in strain [24-25]. Also, FWHM decreases with the annealing temperature.

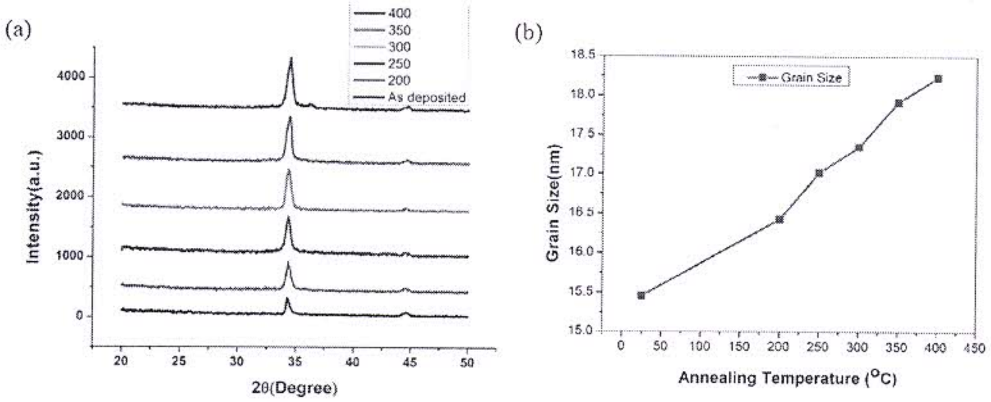

Fig. 2. (a) XRD patterns of as-deposited and annealed ZnO films and (b) grain size of *ZnO* films annealed at different temperatures.

Figures 2–5 are showing the effect of annealing temperature on various microstructural parameters such as grain size *(S)*, dislocation density *(D)* and stress (σ). Grain size *(S)* is calculated using the *Scherer* formula [26]:

$$S = 0.94\,\lambda\,B\cos\theta \qquad (1)$$

Where λ is the wavelength of the X-ray used in *XRD* measurements and it is equal to $0.154056nm$, B is the full width at half maxima *(FWHM)* and θ is the Bragg diffraction angle. Therefore, dislocation density can be calculated using the relation [23]:

$$D = \frac{1}{S^2} \qquad (2)$$

Finally, the film stress can be calculated from the relation [23, 27]:

$$\sigma = -233\left(\frac{c}{c - c_o}\right) \qquad (3)$$

Here, c is the lattice parameter of the deposited *ZnO* films and c_o is the unstrained lattice parameter for powder *ZnO* $(c_o = 0.5205nm)$ [28]. c can be obtained using the relation [23]:

$$c = \frac{\lambda}{\sin\theta} \qquad (4)$$

Grain size increased from $15.46nm$ to $18.24nm$ as shown in Fig. 2(b). In the graph, the value at $25^o\ C$ indicates the grain size of as-deposited *ZnO* (i.e. room temperature deposited) film. The increase in grain size is due to the recrystallization of the thin film [29]. Surface roughness for an as-deposited *ZnO* film was high $\sim 4.42nm$ as shown in Fig. 3(a). However, when the annealing temperature was increased upto 350^oC, the rms roughness became very low ~2.67nm (Fig. 3(b)). On further increasing the annealing temperature to 400^oC, the value rms roughness increased to $3.79nm$ (Fig. 4).

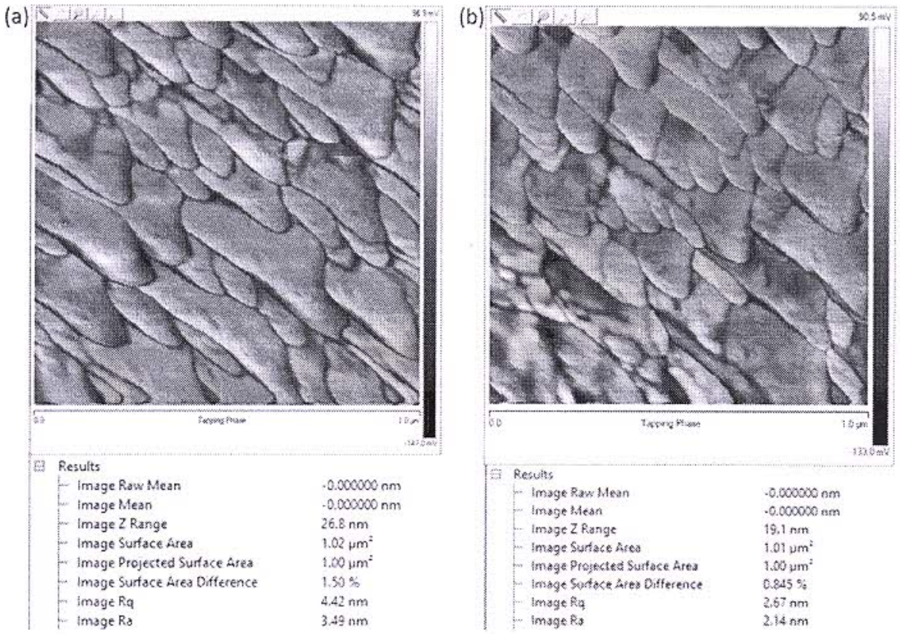

(a)

Results

Image Raw Mean	-0.000000 nm
Image Mean	-0.000000 nm
Image Z Range	26.8 nm
Image Surface Area	1.02 µm²
Image Projected Surface Area	1.00 µm²
Image Surface Area Difference	1.50 %
Image Rq	4.42 nm
Image Ra	3.49 nm

(b)

Results

Image Raw Mean	-0.000000 nm
Image Mean	-0.000000 nm
Image Z Range	19.1 nm
Image Surface Area	1.01 µm²
Image Projected Surface Area	1.00 µm²
Image Surface Area Difference	0.845 %
Image Rq	2.67 nm
Image Ra	2.14 nm

Fig. 3. *AFM* images of (a) as-deposited and (b) annealed *ZnO* film.

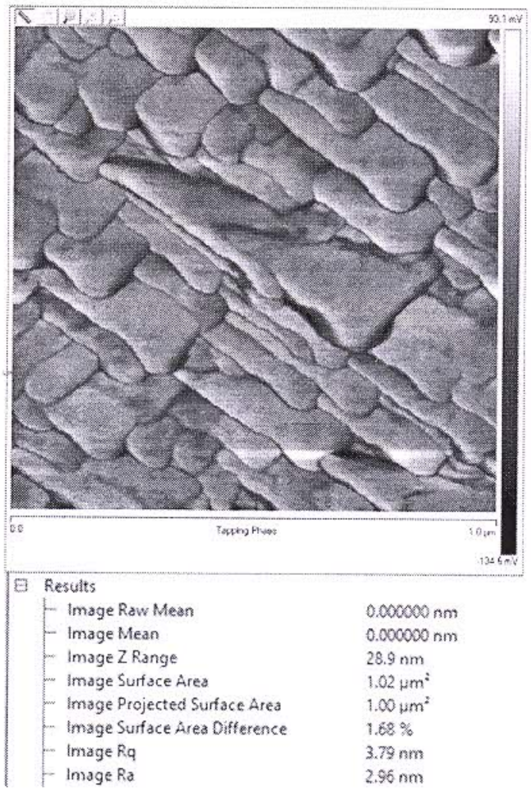

Results

Image Raw Mean	0.000000 nm
Image Mean	0.000000 nm
Image Z Range	28.9 nm
Image Surface Area	1.02 µm²
Image Projected Surface Area	1.00 µm²
Image Surface Area Difference	1.68 %
Image Rq	3.79 nm
Image Ra	2.96 nm

Fig. 4. AFM image of ZnO film annealed at 40 $0^{o}C$.

The reduction in the roughness which takes place initially with the increase in annealing temperature can occur due to the island coalescence process induced from thermal treatment [23, 30]. Sharma et al. [23] argued that due to the presence of some *Frenkel* defects such as *Zn* interstitials and oxygen vacancies at the grain boundaries of deposited films, the coalescence process gets enhanced to make larger grains at higher annealing temperature. However, roughness increases with additional increase in annealing temperature due to further grain growth [22, 26]. The low amount of roughness at 350°C is indicative of smaller acoustic losses in ZnO thin film which is an essential characteristic for acousto-electric applications [31].

Dislocation density has shown a decreasing trend with increasing annealing temperature as depicted in Fig. 5(a). Dislocation density for the as-deposited film is $4.186 \times 10^{-3}\ nm^{-2}$. However, it decreases to a value of $3.704 \times 10^{-3} nm^{-2}$ at the annealing temperature of $20\,0\ ^{o}C$ and further decreases to of $3.006 \times 10^{-3} nm^{-2}2$ at the temperature of $40\ 0\ ^{o}C$. They opined that due to the movement of *Zn* interstitials towards the grain boundaries leads to the reduced concentration of lattice imperfections. This may cause the reduction in dislocation density at higher annealing temperature. Lower dislocation density indicates better crystalline quality of the deposited thin film. For simplicity, the as-deposited values are not shown in graphs of dislocation density and stress.

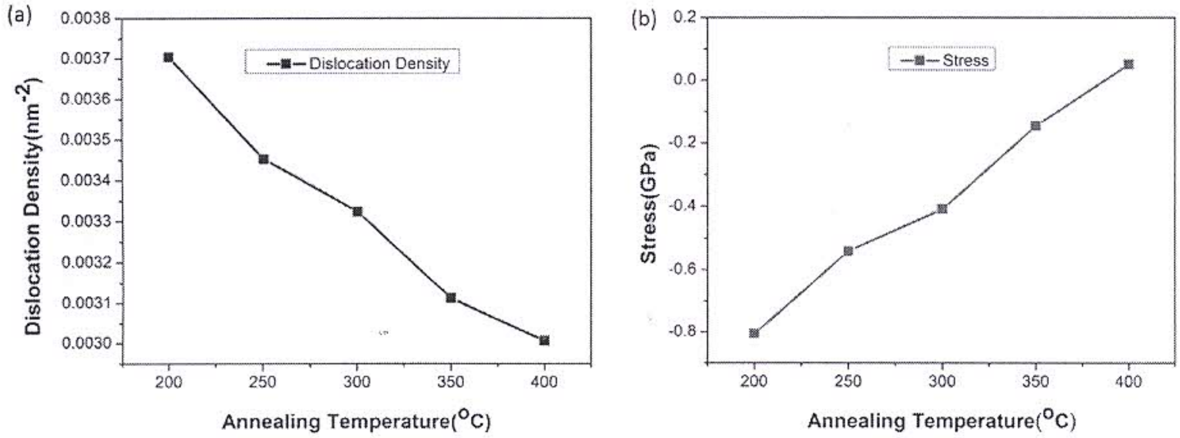

Fig.5. (a) Dislocation density and (b) stress as functions of annealing temperature

Film stress decreases from the as-deposited film value of -1.0036GPa to -0.80516GPa at the annealing temperature of $200^{o}C$. It further decreases to $-0.14615GPa$ at the annealing temperature of $350^{o}C$ as shown in Fig.5(b). The negative sign indicates the presence of compressive stress. At lower annealing temperature, the stress is compressive in nature. The presence of the compressive stress in the as-deposited ZnO films provides a driving force for grain growth during post-deposition annealing [24]. As annealing temperature increases, the film has started to show tensile nature of the stress and at the temperature of $400^{o}C$, it shows a low tensile stress of $0.050798GPa \cong 50.8kPa$. The compressive nature of the stress at lower temperature is due to presence of *Zn* interstitials. On the other hand, the tensile nature exhibited by the film at higher annealing temperature is due to the domination of oxygen vacancies in the lattice of ZnO crystallites [23]. High crystallinity of *ZnO* thin films with reduced strain and stress facilitates its use in acoustic sensors and in many optoelectronic applications.

4. Conclusion

ZnO thin films of thickness $2.5\mu m$ were deposited using *RF* sputtering technique. All the films were annealed at temperatures ranging from $200-400^{o}$ C in steps of 50^{o} C and effect of changing temperature upon different microstructural properties such as grain size, surface roughness, dislocation density and stress were studied. All deposited films exhibited a strong (002) crystallographic orientation in *XRD* measurements and an increase in the intensity of (002) peak as well as increase in grain size with temperature, indicating enhanced crystallinity. Also, dislocation density decreases. Surface roughness has been determined from *AFM* measurements and it exhibited a very low value of $\sim$ 2.67nm at the temperature 350^{o}C. Stress was also found to decrease with temperature. Moreover, nature of stress for deposited *ZnO* thin films got shifted from compressive to tensile as annealing temperature has increased from $200^{o}C$ to 400^{o} C. A nearly stress free film can be obtained at an optimized temperature of 350°C. Therefore, acoustic sensors fabricated on annealed stress free *ZnO* thin film can achieve high sensitivity. They can be utilized in the detection of sound pressure levels in launch vehicles, jet engines etc.

Acknowledgement

The authors thank Director, CSIR-CEERI, Pilani, for encouragement and guidance. Authors also thank Mr. Sanjeev Kumar, Senior Scientist, CSIR-CEERI, for *AFM* measurements and Mr. Deepak Kumar Panwar for facilitating the ZnO deposition. The authors acknowledge the research project (Ref. no. EMR/2017/005107) funded by Science & Engineering Research Board (SERB), DST, Govt. of India for the financial support in carrying out this work.

References

[1] E. S. Kim, R. S. Muller, P. R. Gray, Integrated microphone with CMOS circuits on a single chip, Technical Digest - International Electron Devices Meeting (1989), pp.880-883.

[2] S. S. Lee, R. P. Ried, R. M. White, Piezoelectric cantilever microphone and microspeaker, Journal of Microelectromechanical Systems 5 (4) (1996), pp.238-242.

[3] T.-L. Ren, L.-T. Zhang, L.-T. Liu, Z.-J. Li, Design of a new ferroelectrics silicon integrated microphone and microspeaker, in: ISAF 2000. Proceedings of the 2000 12th IEEE International Symposium on Applications of Ferroelectrics (IEEE Cat. No.00CH37076), Vol. 2, 2000, pp. 885-888.

[4] S. Choon Ko, Y. Chul Kim, S. Seob Lee, Seung Ho Choi, R. K. Sang, Micromachined piezoelectric membrane acoustic device, Sensors and Actuators A 103 (2003), pp.130-134.

[5] R. G. Polcawich, M. Scanlon, J. Pulskamp, J. Clarkson, J. Conrad, D. Washington, R. Piekarz, S. Trolier-Mckinstry, M. Dubey, Design and fabrication of a lead zirconate titanate (PZT) thin film acoustic sensor, Integrated Ferroelectrics 54 (November 2014) (2003), pp. 595-606.

[6] W. S. Lee, S. S. Lee, Piezoelectric microphone built on circular diaphragm, Sensors and Actuators, A: Physical 144 (2) (2008), pp. 367-373.

[7] J. Segovia-Fernandez, S. Sonmezoglu, S. T. Block, Y. Kusano, J. M. Tsai, R. Amirtharajah, D. A. Horsley, Monolithic piezoelectric Aluminum Nitride MEMS-CMOS microphone, TRANSDUCERS 2017 - 19th International Conference on Solid-State Sensors, Actuators and Microsystems (2017), pp.414-417.

[8] A. Rahaman, A. Ishfaque, H. Jung, B. Kim, Bio-inspired rectangular shaped piezoelectric mems directional microphone, IEEE Sensors Journal 19 (1) (2019), pp.88-96.

[9] W. R. Ali, M. Prasad, Design and fabrication of microtunnel and Si diaphragm for ZnO based MEMS acoustic sensor for high SPL and low frequency application, Microsystem Technologies 21 (6) (2015), pp.1249-1255.

[10] Y. Li, Y. Q. Fu, S. D. Brodie, M. Alghane, A. J. Walton, Enhanced micro-droplet splitting, concentration, sensing and ejection by integrating ElectroWetting-On-Dielectrics and Surface Acoustic Wave technologies, 2011 16th International Solid-State Sensors, Actuators and Microsystems Conference, TRANSDUCERS'11 (2011), pp.2936-2939.

[11] W. R. Ali, M. Prasad, Piezoelectric mems based acoustic sensors: A review, Sensors and Actuators A: Physical 301 (2020) 111756.

[12] F. U. Hamelmann, Thin film zinc oxide deposited by CVD and PVD, Journal of Physics: Conference Series 764 (1) (2016) pp.0-8.

[13] A. Kumar, M. Prasad, V. Janyani, R. P. Yadav, Design, fabrication and reliability study of piezoelectric zno based structure for development of mems acoustic sensor, Microsystem Technologies (2019), pp.1-12.

[14] J. P. Atanas, R. Al Asmar, A. Khoury, A. Foucaran, Optical and structural characterization of ZnO thin films and fabrication of bulk acoustic wave resonator (BAW) for the realization of gas sensors by stacking ZnO thin layers fabricated by e-beam evaporation and rf magnetron sputtering techniques, Sensors and Actuators, A: Physical 127 (1) (2006), pp.49-55.

[15] H. Fazmir, Y. Wahab, A. Anuar, M. Zainol, M. Najmi, M. Mazalan, M. Md Arshad, Properties of Piezoelectric Layer Deposited by Sol-Gel Method for MEMS Sensor Applications, Applied Mechanics and Materials 780 (2015), pp.23-27.

[16] L. Znaidi, Sol-gel-deposited ZnO thin films: A review, Materials Science and Engineering B: Solid-State Materials for Advanced Technology 174 (1-3) (2010) pp.18-30.

[17] B. P. Zhang, K. Wakatsuki, N. T. Binh, N. Usami, Y. Segawaa, Effects of growth temperature on the characteristics of zno epitaxial films deposited by metalorganic chemical vapor deposition, Thin Solid Films 449 (2004), pp.12-19.

[18] J. W. Hoon, K. Y. Chan, J. Krishnasamy, T. Y. Tou, D. Knipp, Direct current magnetron sputter-deposited ZnO thin films, Applied Surface Science 257 (7) (2011), pp.2508-2515.

[19] M.-C. Pan, T.-H. Wu, B. Tuan Anh, W.-C. Shih, Fabrication of highly c-axis textured zno thin films piezoelectric transducers by rf sputtering, Journal of Materials Science-materials in Electronics - J Mater Sci-Mater Electron 23 (02 2012).

[20] A. Cimpoiasu, N. M. van der Pers, T. H. de Keyser, A. Venema, M. J. Vellekoop, Stress control of piezoelectric ZnO films on silicon substrates, Smart Materials and Structures 5 (6) (1996) , pp.744-750.

[21] M. D. Williams, Development of a mems piezoelectric microphone for aeroacoustic applications, Phd thesis, University of Florida (2011).

[22] Z. Fang, Z. Yan, Y. Tan, X. Liu, Y. Wang, Influence of post-annealing treatment on the structure properties of zno films, Applied Surface Science 241 (2005), 303-308.

[23] S. Sharma, T. Varma, K. Asokan, C. Periasamy, D. Boolchandani, Annealing temperature dependent structural and optical properties of rf sputtered zno thin films, Journal of Nanoscience and Nanotechnology 17 (2017), pp.300-305.

[24] T. Hiramatsu, M. Furata, H. Furata, T. Matsuda, T. Hirao, Influence of thermal annealing on microstructures of zinc oxide films deposited by rf magnetron sputtering, Japanese Journal of Applied Physics 46 (6A) (2007), pp.3319-3323.

[25] M. Puchert, P. Timbrell, R. Lamb, Postdeposition annealing of radio frequency magnetron sputtered zno films, J. Vac. Sci. Technol. A 14 (4) (1996), 2220-2230.

[26] G. P. Daniel, V. Justinvictor, P. B. Nair, K. Joy, P. Koshy, P. Thomas, Effect of annealing temperature on the structural and optical properties of zno thin films prepared by rf magnetron sputtering, Physica B 405 (2010), pp.1782-1786.

[27] D. Rusu, G. Rusu, D. Luca, Structural characteristics and optical properties of thermally oxidized zinc films, ACTA PHYSICA POLONICA A 119 (6) (2011), pp. 850-856.

[28] Powder diffraction file, jcpds , pp.36-1451.

[29] H. et al., Influence of annealing temperature on the properties of zno thin films grown by sputtering, in: Energy Procedia, Vol. 25, 2011, pp.55-61.

[30] K.-H. Bang, D.-K. Hwang, J.-M. Myoung, Effects of zno buffer layer thickness on properties of zno thin films deposited by radio-frequency magnetron sputtering, Applied Surface Science 207 (2003), pp.359-364.

[31] M. Assouar, M. El Hakiki, O. Elmazria, P. Alnot, C. Tiusan, Synthesis and microstructural characterisation of reactive rf magnetron sputtering aln films for surface acoustic wave filters, Diamond and Related Materials 13 (4) (2004) pp.1111-1115, 14th European Conference on Diamond, Diamond-Like Materials, Carbon Nanotubes, Nitrides and Silicon Carbide.